ELSEVIER

Journal of Non-Crystalline Solids 293–295 (2001) 726–730

JOURNAL OF NON-CRYSTALLINE SOLIDS

www.elsevier.com/locate/jnoncrysol

High-resolution atomic distribution functions of disordered materials by high-energy X-ray diffraction

V. Petkov [a,*], S.J.L. Billinge [a], S.D. Shastri [b], B. Himmel [c]

[a] *Department of Physics and Astronomy, Center for Fundamental Materials Research, Michigan State University, East Lansing, MI 48823, USA*

[b] *Advanced Photon Source, Argonne National Laboratory, Argonne, IL 60439, USA*

[c] *FB Elektrotechnik and Informationtechnik, Universität Rostock, Rostock, Germany*

Abstract

The atomic-scale structure of materials with different degrees of structural disorder has been investigated by high-energy ($E \geqslant 60$ keV) X-ray diffraction. Good quality structure functions extended to wave vectors of magnitude $Q \geqslant 40$ Å^{-1} have been obtained even in case of materials composed of weakly scattering, light atomic species. The corresponding high-resolution atomic distribution functions allowed fine structural features differing in as little as (0.14 Å) to be resolved. In particular, the distinct Ga–As (~2.43 Å) and In–As (2.61 Å) bonds in In–Ga–As alloys have been differentiated. The atomic-scale structure of 'restacked' WS_2 has been determined and the presence of three distinct W–W distances occurring at 2.77, 3.27 and 3.85 Å established. Finally, Si–O (~1.61 Å), Al–O (~1.75 Å) and Ca–O (~2.34 Å) bonds in calcium aluminosilicate glasses have been differentiated and the characteristics of the respective co-ordination polyhedra revealed.

1. Introduction

Knowledge of the atomic-scale structure is a prerequisite to understanding the physical properties and technological characteristics of materials. Also, many technologically important materials contain significant disorder on the atomic scale. Often this disorder has a direct effect on the properties which make the material technologically and/or scientifically important. It is clearly advantageous to characterize the structure of disordered materials with high resolution. A fruitful experimental approach is the combination of the high-energy X-ray diffraction and the atomic pair distribution function (PDF) technique.

The atomic PDF, $G(r) = 4\pi r[\rho(r) - \rho_0]$, is the sine Fourier transform of the experimentally observable total structure function, $S(Q)$, i.e.,

$$G(r) = (2/\pi) \int_{Q=0}^{Q_{\max}} Q[S(Q) - 1] \sin(Qr)\, \mathrm{d}Q, \qquad (1)$$

where r is the radial distance, Q the magnitude of the wave vector and $\rho(r)$ and ρ_0 the local and average atomic number densities, respectively. The structure function is related to the elastic part of the total diffracted intensity, $I^{\mathrm{el}}(Q)$, as follows:

* Corresponding author. Tel.: +1-517 353 4500; fax: +1-517 353 5288.

E-mail address: petkov@pa.msu.edu (V. Petkov).

0022-3093/01/$ - see front matter
PII: S0022-3093(01)00864-X

$$S(Q) = 1 + \left[I^{\mathrm{el}}(Q) - \sum c_i |f_i(Q)|^2\right] \Big/ \left|\sum c_i f_i(Q)\right|^2, \quad (2)$$

where c_i and f_i are the atomic concentration and scattering factor, respectively, for the atomic species of type i [1]. Two important advantages of the atomic PDFs are to be noted. First, the PDF is obtained with no assumption of periodicity and, therefore, glassy materials as well as polycrystals exhibiting different degrees of structural disorder can be studied applying the same approach. Second, by using high-energy X-rays high values of Q can be assessed. This results in PDFs with improved resolution allowing quite fine structural features to be revealed. The advantages are well demonstrated by the results presented below.

2. Examples of high-energy X-ray diffraction experiments

2.1. Local structural disorder in In–Ga–As semiconductor alloys

$In_xGa_{1-x}As$ alloys are technologically important because they allow the semiconductor band gap to be varied continuously between the band gap values of the end members by varying the composition, x. XAFS experiments [2] have shown that In–As and Ga–As bond lengths do not take average values but remain close to their natural lengths $L_{\mathrm{Ga–As}} = 2.43$ Å and $L_{\mathrm{In–As}} = 2.61$ Å in the alloy. Accordingly, the underlying zinc-blende lattice must distort significantly to accommodate the two distinct bond lengths in the alloys. Since the structural distortion affects the alloy's properties it warrants a detailed study. The study was carried out at the A2 beam line, The Cornell high-energy synchrotron source (CHESS), using X-rays of energy 60 keV [3]. Two of the extended structure functions obtained are shown in Fig. 1. Significant Bragg scattering (well-defined peaks) is present up to $Q \sim 35$ Å^{-1} in the end member GaAs. The material has a perfect crystalline order. The Bragg peaks disappear at much lower Q values in the $In_{0.5}Ga_{0.5}As$ sample. At high-Q values, only oscillating diffuse scattering is seen. The alloy obviously exhibits considerable structural disorder. The two different bond lengths that cause it are well seen as a split first peak in the corresponding $G(r)$ also shown in Fig. 1. To quantify the structural distortions in the alloy, simple models based on the 8-atom unit cell of the zinc-blende lattice were fit to the experimental PDFs [4]. The PDF for GaAs fits well with a model based on the perfect zinc-blende structure as can be seen in Fig. 1. However, definitive static displacement of the atoms from their sites in the ideal zinc-blende lattice were necessary to be introduced in the model structure to fit the PDF for $In_{0.5}Ga_{0.5}As$. The refined discrete displacements on As and metal (In;Ga) sites amounted to 0.133(5) and 0.033(8) Å, respectively. Fragments of the refined structure

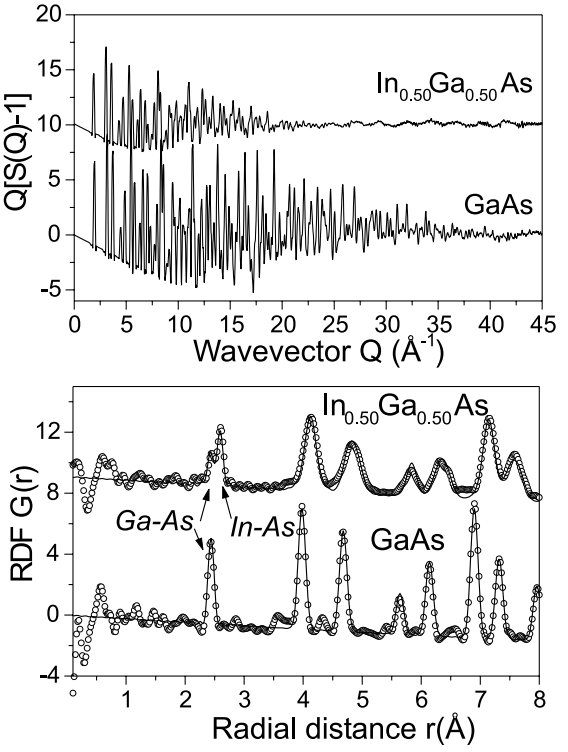

Fig. 1. Reduced structure functions $Q[S(Q) - 1]$ (upper part) and the corresponding high-resolution atomic PDFs (symbols; lower part) for GaAs and $In_{0.5}Ga_{0.5}As$. Model PDFs (full line; lower part) are based on perfect (for GaAs) and distorted (for $In_{0.5}Ga_{0.5}As$) zinc-blende lattices.

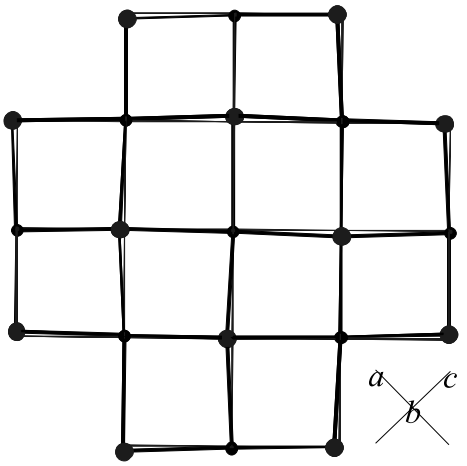

Fig. 2. Schematic representation of the local structural distortions in $In_{0.5}Ga_{0.5}As$. Fragments of the perfect lattice (thin line) can be compared with the distorted one (thick line). The view is a projection along the *b* axis of the unit cell. The large circles are As sites and the small circles the metal (In;Ga) sites.

models are illustrated in Fig. 2. The model result shows that in In–Ga–As alloys most of the structural distortion occurs by arsenic moving off its site, but displacement of metal atoms is also important [3,4].

2.2. Structure of restacked WS_2

Layered WS_2 shows fascinating chemical properties. It can be easily exfoliated to form a suspension of single (WS_2) layers and then restacked, with foreign species included if desired [5]. X-ray diffraction experiments were carried out to determine the structure of restacked WS_2 since it would help in understanding the material's guest–host and catalytic properties. The experiments were carried out at the A2 beam line, CHESS, using X-rays of energy 60 keV. A complementary experiment on pristine WS_2 was also carried out with the use of laboratory source of X-rays with Ag anode. The experimental structure functions and atomic PDFs obtained are shown in Fig. 3. The structure function of pristine WS_2 consists of well-defined Bragg peaks – a characteristic typically seen in well-crystalline materials. The corresponding atomic PDF perfectly fits with the well-known structure of hexagonal WS_2 [6]. The structure function of restacked WS_2 contains only a few sharp peaks and a pronounced diffuse component – a characteristic of a significantly disordered material. Such a featureless experimental structure function is practically impossible to be tackled by ordinary techniques for structure determination including the Rietveld technique. The corresponding PDF, however, is rich in structure-related features and lends itself to structure determination. Several structure models were tested and it was found that the structure of restacked WS_2 is best described on the basis of a monoclinic unit cell being a distorted derivative of the 8-atom unit cell of orthorhombic WTe_2 [6]. The quality of this structure model is well demonstrated in Fig. 3. A fragment of it is given in Fig. 4. Thus, it was found that although restacked WS_2 is quite disordered it still possesses three-dimen-

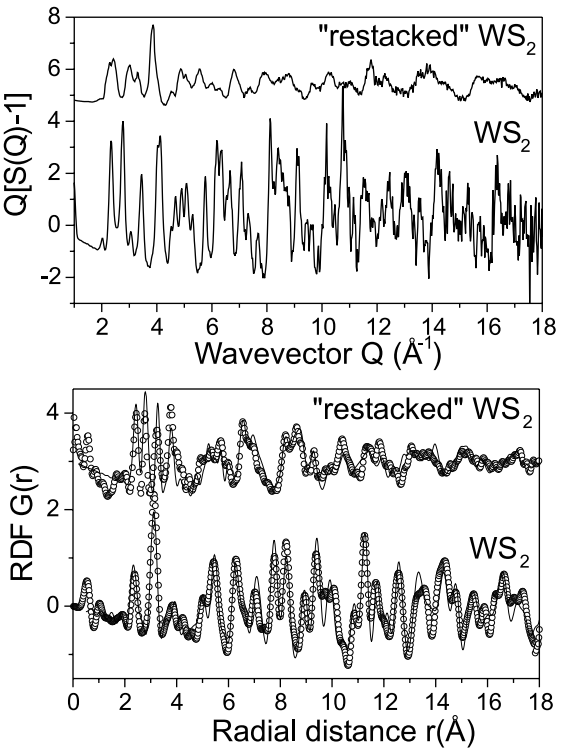

Fig. 3. Reduced structure functions $Q[S(Q) - 1]$ (upper part) and the corresponding atomic PDFs (symbols; lower part) for pristine and restacked WS_2. Model PDFs (full line; lower part) are based on hexagonal (for pristine WS_2) and monoclinic (for restacked WS_2) structures as described in the text.

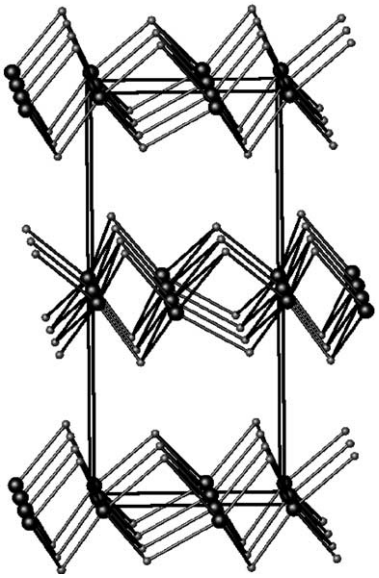

Fig. 4. Fragment of the structure of restacked WS_2 with the monoclinic unit cell shown. The big circles are W atoms and the small ones are S atoms.

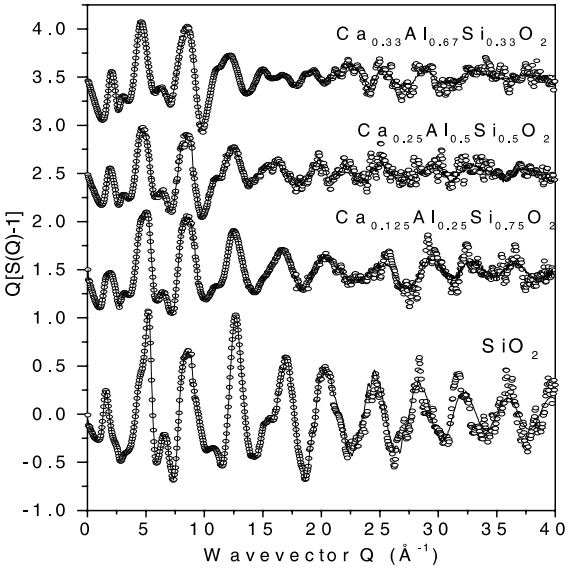

Fig. 5. Reduced structure functions $Q[S(Q) - 1]$ for calcium aluminosilicate glasses (symbols) together with the optimum smooth line placed with the help of the maximum entropy method [9].

sional order, i.e., it is not simply a turbostratic pile-up of (WS_2) monolayers. The structures of pristine and restacked WS_2 differ most in the spatial arrangement of metal atoms. Tungsten atoms occupy a single site and are separated by the same distance of 3.18 Å in pristine WS_2. They occupy two distinct sites in restacked WS_2. As a result three distinct W–W atomic-pair distances occur at 2.77, 3.85 and 3.27 Å, respectively [7]. These distinct W–W pairs are what make the low-r region of the PDF for restacked WS_2 look so different from the one of the PDF for pristine WS_2 (see Fig. 3).

2.3. Polyhedral units and network connectivity in calcium aluminosilicate glasses

Silicate glasses in general, and calcium aluminosilicates glasses in particular, are of great industrial and technological importance. It is well known that silica glass is a continuous network of corner-shared SiO_4 tetrahedra. When Si^{4+} is replaced by Al^{+3} and Ca^{+2} is introduced to balance the charge the glassy structure changes. The

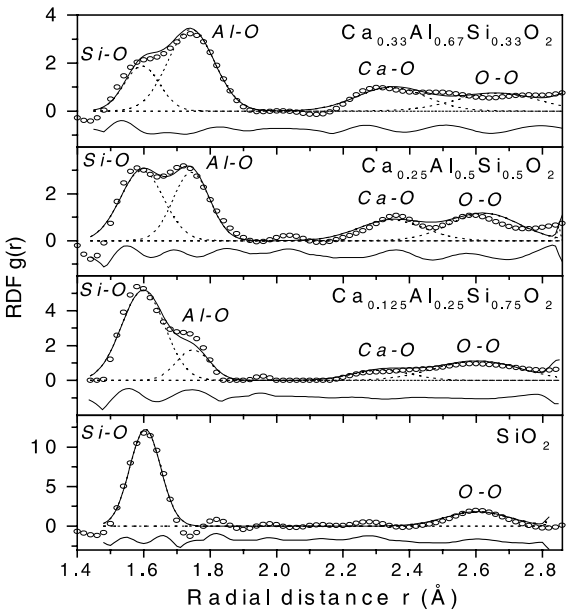

Fig. 6. Gaussian fit to the first peaks in the atomic PDFs, $G(r) = \rho(r)/\rho_0$, for $Ca_{x/2}Al_xSi_{1-x}O_2$ glasses ($x = 0$, 0.25, 0.5, 0.67). Experimental data – symbols; fitted data – full line; individual Gaussians – broken line; residual difference – full line (bottom). Peaks are labeled with the corresponding atomic pairs.

change involves a replacement of Si–O polyhedra by Al–O ones and an emerging of so-called non-bridging oxygens (NBO) linking an Si–O or Al–O unit with a Ca–O one [8]. Important issues about the modifier (Ca) ion co-ordination and the nature of NBOs that break the network are, however, not so well established. To fill this gap a study on the atomic ordering in a series of $Ca_{x/2}Al_xSi_{1-x}O_2$ glasses ($x = 0$, 0.25, 0.5, 0.67) was undertaken. The experiments were carried out at the 1-ID beam line, The Advanced Photon Source, Argonne, with the use of X-rays of energy 80.6 keV. The structure functions obtained are shown in Fig. 5. They exhibit prominent oscillations up to the maximum Q value of 40 $\mathring{A}^{-1}$ reached. The oscillations may only come from the presence of well-defined polyhedral units building the glasses. These polyhedra are seen as well-defined peaks in the low-r region of the experimental PDFs shown in Fig. 6. By fitting the peaks with Gaussians the corresponding co-ordination numbers and radii were estimated. It is found that both Si and Al are co-ordinated by four oxygens and thus participate in a continuous tetrahedral network when Al/Ca content is low ($x = 0$, 0.25). By $x = 0.5$ the network begins to break. It is indicated by the slight drop in the *average* co-ordination number of Si from 4.0(1) to 3.85(1). When more than half of Si is replaced by Al ($x = 0.67$) the number of NBOs in the first co-ordination sphere of Si increases making the *average* Si–O co-ordination number as low as 3.2(1). The Al–O average co-ordination number is found to be close to 4.0(1) for all values of x. Thus Al–O tetrahedra are always free of NBOs and fully integrated in the network. Ca–O co-ordination is found to be well defined and close to 5.2(1) for all values of x. The result implies that not only Si/Al–O tetrahedra but Ca polyhedra, too, play a role in the formation of the glassy structure [10].

3. Conclusion

Good quality, high-resolution atomic PDFs can be obtained by high-energy X-ray diffraction even in case of materials composed of weakly scattering, light atomic species. Thus the structure of materials exhibiting different degrees of structural disorder can be studied with improved resolution. These could be crystalline materials such as In–Ga–As alloys where a small deviation from the perfect order is present, heavily disordered but still three-dimensionally periodic materials such as re-stacked WS_2 and completely disordered materials such as calcium aluminosilicate glasses. High-resolution PDFs are expected to become more frequently employed in structure studies with the number of synchrotron sources rapidly increasing worldwide.

Acknowledgements

The semiconductor alloy work was supported by DOE grant DE FG02 97ER45651 and the WS_2 and glasses work by NSF grant CHE 99-03706. CHESS is operated by NSF through grant DMR97-13242. The Advanced Photon Source is operated by DOE under contract W-31-109-Eng-38. Thanks are due to S. Kycia, I-K. Jeong, F. Muhiuddin-Jacobs, Th. Proffen, J. Heising and M. Kanatzidis for the fruitful cooperation.

References

[1] B.E. Warren, X-ray Diffraction, Dover, New York, 1990.
[2] J.C. Mikkelson, J.B. Boyce, Phys. Rev. Lett. 49 (1982) 1412.
[3] V. Petkov, I-K. Jeong, J.S. Chung, M.F. Thorpe, S. Kycia, S.J.L. Billinge, Phys. Rev. Lett. 83 (1999) 4089.
[4] V. Petkov, I-K. Jeong, F. Muhiuddin-Jacobs, T.h. Proffen, J.S.L. Billinge, W. Dmowski, J. Appl. Phys. 88 (2000); V. Petkov, S.J.L. Billinge, Physica B 305 (2001) 83.
[5] W.M.R. Divigalpitiya, R.F. Frindt, S.R. Morrison, Science 246 (1989) 369.
[6] R.W.G. Wyckoff, Crystal Structures, Wiley, New York, 1964.
[7] V. Petkov, S.J.L. Billinge, J. Heising, M. Kanatzidis, J. Am. Chem. Soc. 122 (2000) 11571.
[8] B.O. Mysen, Structure and Properties of Silicate Melts, Elsevier, Amsterdam, 1988.
[9] V. Petkov, R. Danev, J. Appl. Crystallogr. 31 (1998) 609.
[10] V. Petkov, S.J.L. Billinge, S.D. Shastri, B. Himmel, Phys. Rev. Lett. 85 (2000) 3436.